Cantharidin induces apoptosis of H460 human lung cancer cells through mitochondria-dependent pathways

TE-CHUN HSIA[1,2], CHIEN-CHIH YU[3], SHU-CHUN HSU[4], NOU-YING TANG[1], HSU-FENG LU[5], YI-PING HUANG[6], SHIN-HWAR WU[7], JAUNG-GENG LIN[1] and JING-GUNG CHUNG[4,8]

[1]Graduate Institute of Chinese Medicine, China Medical University; [2]Department of Internal Medicine, China Medical University Hospital; [3]School of Pharmacy, [4]Department of Biological Science and Technology, China Medical University, Taichung; [5]Department of Clinical Pathology, Cheng Hsin General Hospital, Taipei; [6]Department of Physiology, China Medical University, Taichung; [7]Division of Critical Care Medicine, Department of Medicine, Changhua Christian Hospital, Changhua; [8]Department of Biotechnology, Asia University, Taichung, Taiwan, R.O.C.

Received February 14, 2014; Accepted April 25, 2014

DOI: 10.3892/ijo.2014.2428

Abstract. Lung cancer is one of the leading causes of death in cancer-related diseases. Cantharidin (CTD) is one of the components of natural mylabris (*Mylabris phalerata* Pallas). Numerous studies have shown that CTD induced cytotoxic effects on cancer cells. However, there is no report to demonstrate that CTD induced apoptosis in human lung cancer cells. Herein, we investigated the effect of CTD on the cell death via the induction of apoptosis in H460 human lung cancer cells. Flow cytometry assay was used for examining the percentage of cell viability, sub-G1 phase of the cell cycle, reactive oxygen species (ROS) and Ca^{2+} productions and the levels of mitochondrial membrane potential ($\Delta\Psi_m$). Annexin V/PI staining and DNA gel electrophoresis were also used for examining cell apoptosis. Western blot analysis was used to examine the changes of apoptosis associated protein expression and confocal microscopy for examining the translocation apoptosis associated protein. Results indicated that CTD significantly induced cell morphological changes and decreased the percentage of viable H460 cells. CTD induced apoptosis based on the occurrence of sub-G1 phase and DNA fragmentation. We found that CTD increased gene expression (mRNA) of caspase-3 and -8. Moreover, CTD increased ROS and Ca^{2+} production and decreased the levels of $\Delta\Psi_m$. Western blot analysis results showed that CTD increased the expression of cleavage caspase-3 and -8, cytochrome *c*, Bax and AIF but inhibited the levels of Bcl-xL. CTD promoted ER stress associated protein expression such as GRP78, IRE1α, IRE1β, ATF6α and caspase-4 and it also promoted the expression of calpain 2 and XBP-1, but inhibited calpain 1 that is associated with apoptosis pathways. Based on those observations, we suggest that CTD may be used as a novel anticancer agent for the treatment of lung cancer in the future.

Correspondence to: Dr Jing-Gung Chung, Department of Biological Science and Technology, China Medical University, No. 91, Hsueh-Shih Road, Taichung 40402, Taiwan, R.O.C.
E-mail: jgchung@mail.cmu.edu.tw

Dr Jaung-Geng Lin, Graduate Institute of Chinese Medicine, China Medical University, No. 91, Hsueh-Shih Road, Taichung 40402, Taiwan, R.O.C.
E-mail: jglin@mail.cmu.edu.tw

Key words: cantharidin, mitochondria, sub-G1 phase, apoptosis, H460 cells

Introduction

Lung cancer is the major cause of death in cancer-related disease in the developed world. It was estimated that about 1.2 million new cases are diagnosed each year worldwide, and of those patients with lung cancer, over 1 million die annually (1). In Taiwan, it is the leading type of cancer causing death; the reports in 2010 from the Department of Health (Taiwan) indicated that 36.8 individuals per 100,000 die annually from lung cancer in Taiwan. The treatment of patients with lung cancer includes surgical resection, chemotherapy, radiation or the combinations of chemotherapy and radiation (2,3). However, the outcome remains unsatisfactory.

The dried body of mylabris (*Mylabris phalerata* Pallas) was reported to treat malign sores and to relieve blood stasis in the Chinese population (2,3). CTD, a terpenoid, is one of the compounds from mylabris, and has been shown to induce apoptosis in murine erythroleukemia cells (4), human hepatocellular carcinoma cells (5), human multiple myeloma cells (6), human pancreatic cancer cell lines (7,8), human bladder carcinoma cell line (9,10), breast cancer cells (11) and human colon cancer cells (12). It was reported that CTD is a potent and selective inhibitor of protein phosphatase 2A (PP2A) (8). In human bladder carcinoma cell line, CTD induced secondary necrosis and COX-2 overexpression (8)

and in rat, CTD induces cystitis through c-Fos and COX-2 overexpression (13).

Recently, in patients with molluscum contagiosum, they were treated with CTD and experienced minimal side effects and provided important prospective safety data (14). Moreover, in primary hepatoma, CTD and its analogs have shown therapeutic effects in clinical trials, while these effects include cases at the advanced stage without the suppression of the bone marrow (15). Although numerous studies have shown that CTD can induce cytotoxic effects in many cancer cell lines, however, there is now reports to show that CTD affects human lung cancer cells, thus, in the present study, we investigated the cytotoxic effects of CTD on human lung cancer H460 cells and we found that CTD induced cell death through the induction of apoptosis *in vitro*.

Materials and methods

Chemicals and reagents. CTD, dimethyl sulfoxide (DMSO), 4',6-diamidino-2-phenylindole (DAPI), propidium iodide (PI) and Trypsin-EDTA were obtained from Sigma Chemical Co. (St. Louis, MO, USA). Minimum essential medium (MEM), fetal bovine serum (FBS), L-glutamine and penicillin-streptomycin were purchased from Gibco®/Invitrogen Life Technologies (Carlsbad, CA, USA). Primary antibody against caspase-3, cleaved caspase-4, cleaved caspase-8, AIF, Bax, Bcl-xL, cytochrome *c*, GRP78, IRE1α, IRE1β, ATF6α, calpain 1, calpain 2, XBP-1 and peroxidase conjugated secondary antibodies were purchased from Cell Signaling Technology, Inc. (Beverly, MA, USA). The enhanced chemiluminescence (ECL) detection system was obtained from Amersham Life Sciences, Inc. (Arlington Heights, IL, USA).

Cell culture. The human lung cancer cell line (H460 cells) was purchased from the Food Industry Research and Development Institute (Hsinchu, Taiwan). Cells were cultured in RPMI-1640 supplemented with 10% heat inactivated FBS, 100 U/ml penicillin, 100 μg/ml streptomycin, and 2 mM L-glutamine in a 75-cm^2 tissue culture flasks at 37˚C under 5% CO_2 in humidified air.

Cell morphology and viability, cell cycle distribution and sub-G1 assays. H460 cells (2x10^5 cells/well) were cultured in 12-well plates for 24 h then treated with CTD at various concentrations (0, 5, 7.5, 10, 15, 30 μM) or 0.5% DMSO as a vehicle control for 24 and 48 h. For cell morphological examinations, cells in the wells were examined and photographed under contrast phase microscopy. For total viable cell measurements, cells in each well were harvested, counted and stained with PI (5 μg/ml) and then were analyzed by using flow cytometry (FACSCalibur, BD Biosciences, San Jose, CA, USA) assay as previously described (15). For cell cycle distribution and sub-G1 phase determinations, all harvested cells from each well were washed with phosphate buffer solution (PBS), incubated with RNase A (50 μg/ml) for 30 min, and were stained with PI (50 μg/ml) for 5 min, and analyzed for cell cycle distribution including sub-G1 phase by using flow cytometry system (Becton-Dickinson, San Jose, CA, USA). The percentages of cells in different phases of the cell cycle were analyzed by using the ModFit LT 3.0 program (Verity Software House, ME, USA), as previously described (16).

Annexin V-FITC/PI staining for cell apoptosis. Annexin V-FITC/PI staining method was used to confirm cell apoptosis which were observed in sub-G1 of cell cycle assay. Briefly, H460 cells (2x10^5 cells/well) were treated with CTD for 0, 1, 3 and 6 h. Cells were harvested and washed with PBS, re-suspended in binding buffer (10 mM HEPES/NaOH pH 7.4, 140 mM NaCl, 25 mM $CaCl_2$), and stained with FITC-conjugated Annexin V (Pharmingen, Becton-Dickinson Co., San Diego, CA, USA) for 15 min in the dark, at room temperature and washed with binding buffer. All samples were measured for the Annexin V-FITC/PI fluorescence intensity by flow cytometry as described (17).

DNA fragmentation examination. H460 cells (3x10^5 cells/well) were placed in 6-well plates for 24 h and were treated with CTD of various concentrations (0, 5, 10, 15 μM) for 24 h. DNA samples were isolated by using DNA isolation kit. The isolated DNA (2 μg) was investigated by using DNA gel electrophoresis which was carried out in 0.5% agarose gel in Tris/acetate buffer at 15 V for 2 h as described previously (17). After electrophoresis, ethidium bromide was used to stain the DNA in the gel, and the gel was further examined and photographed by fluorescence microscopy as previously described (18).

Reactive oxygen species (ROS), intracellular Ca^{2+} and mitochondrial membrane potential ($\Delta\Psi_m$) assays. ROS, Ca^{2+} and $\Delta\Psi_m$ measurements were performed by flow cytometry. Briefly, H460 cells (2x10^5 cells/well) were treated with 10 μM of CTD for 0, 1, 3, 6, 12 or 24 h. All cells from each treatment and time point were isolated by centrifugation and then were re-suspended in 500 μl of DCFH-DA (10 μM) for 30 min for further ROS (H_2O_2) measurement, re-suspended in 500 μl of Fluo-3/AM (2.5 μg/ml) for 30 min for further intracellular Ca^{2+} concentrations measurement and re-suspended in 500 μl of $DiOC_6$ (4 μmol/l) for 30 min to further the levels of $\Delta\Psi_m$ measurement. All samples were analyzed by flow cytometry as described (17).

Real-time PCR assay for mRNA levels of caspase-3 and -8. The mRNA expression of caspase-3 and -8 were performed by real-time PCR. Briefly, H460 cells (2x10^5 cells/well) were treated with 10 μM of CTD for 0, 12 and 24 h. Then cells were harvested and total RNA was extracted from each treatment using the Qiagen RNeasy mini kit (Qiagen, Inc., Valencia, CA) as described previously (19). High Capacity cDNA Reverse Transcription Kit (Applied Biosystems, Foster City, CA) was used to reverse-transcribe all RNA samples at 42˚C for 30 min according to the standard protocol of the supplier. The following conditions were used for quantitative PCR: 2 min at 50˚C, 10 min at 95˚C, and 40 cycles of 15 sec at 95˚C, 1 min at 60˚C using 1 μl of the cDNA reverse-transcribed as described above, 2X SYBR-Green PCR Master mix (Applied Biosystems) and 200 nM forward and reverse primers: caspase-3 forward, CAGTGGAGGCCGACTTCTTG and reverse, TGGCACAAA GCGACTGGAT; caspase-8 forward, GGATGGCCACTGTG AATAACTG and reverse, TCGAGGACATCGCTCTCTCA;

GAPDH forward, ACACCCACTCCTCCACCTTT and reverse, TAGCCAAATTCGTTGTCATACC. All assays were performed by Applied Biosystems 7300 real-time PCR system in triplicates and expression fold-changes were derived using the comparative CT method (20,21).

Western blot analysis. H460 cells ($1x10^6$ cells/dish) were placed in 10-cm dish for 24 h then were incubated with 10 μM CTD for 0, 6, 12, 24 and 48 h. After treatment under each experimental condition, total cell lysates were denatured with ice-cold lysis buffer [10 mM Tris-HCl (pH 7.4), 150 mM NaCl, 1 mM EGTA, 0.3 mM PMSF, 0.2 mM sodium orthovanadate, 0.1% SDS, 1 mM EDTA, 1% NP-40, 10 mg/ml leupeptin, and 10 mg/ml aprotinin] and then were centrifuged at 13,000 x g for 10 min at 4˚C (16,17). A Bio-Rad protein assay kit (Hercules, CA, USA) was used for measuring the total protein of each sample. The clarified protein lysates (30 μg) were electrophoretically resolved on denaturing SDS-polyacrylamide gel (12%) followed by transfer onto nitrocellulose membranes, and then blotted with the relevant primary antibodies (anti-caspase-3, caspase-4, caspase-8, AIF, Bax, Bcl-xL, cytochrome *c*, GRP78, IRE1α, IRE1β, ATF6α, calpain 1, calpain 2, XBP-1) overnight at 4˚C followed by peroxidase-conjugated secondary antibody for 1 h at room temperature (25˚C). Finally, proteins were visualized by ECL detection (Amersham Biosciences ECL™) and exposed to X-ray film and bands obtained were quantified using NIH Image analyzer (NIH, Bethesda, MD) (17,18).

Confocal laser scanning microscopy assay. H460 cells ($3x10^5$ cells/well) were placed on 6-well chamber slides and incubated with 10 μM CTD for 24 h. The cells were fixed in 4% formaldehyde in PBS for 15 min followed by using 0.3% Triton X-100 in PBS for 1 h and by using 2% BSA for blocking non-specific binding sites. Then cells were stained by primary antibodies such as anti-cytochrome *c*, anti-AIF and anti-Endo G (all in green fluorescence) overnight. Then cells were washed twice with PBS and were stained with secondary antibody (FITC-conjugated goat anti-mouse IgG) followed PI (red fluorescence) staining for nuclein examination as described previously. Slides with cells were mounted, examined and photo-micrographed under a Leica TCS SP2 Confocal Spectral Microscope as described previously (17,18). Localization of protein in nuclei is demonstrated by the development of orange color due to red and green overlapped pixels.

Statistical analysis. All data were performed and expressed as mean ± SD from triplicate experiments. Statistically significant differences between the CTD-treated and -untreated (control) groups were analyzed by Student's t-test, with values of $^*p<0.05$ considered statistically significant.

Results

CTD induces cell morphological changes and decreases the cell viability of H460 cells. H460 cells were treated with 0, 5, 7.5, 10, 15 and 30 μM of CTD for 24 and 48 h before the cells were examined and photographed for examining the cell morphological changes and were harvested for the percentage of viable cells and the results are shown in Fig. 1. Fig. 1A and B indicate that CTD induced cell morphological changes and led to cell death and debris. CTD led to enhancement of dead cells following 5-30 μM as indicated by white arrows. Furthermore, Fig. 1C shows a significant dose-dependent reduction of living cells with CTD treatment in H460 cells and these effects are dose-dependent.

CTD induces sub-G1 phase and apoptosis of H460 cells. H460 cells were treated with 0, 5, 7.5, 10, 15 and 30 μM of CTD for 24 and 48 h before the cells were examined for sub-G1 phase in cell cycle assay and the results are shown in Fig. 2. Data from Fig. 2A-C indicated that CTD induced sub-G1 phase development, thus CTD induced apoptosis and these effects are dose-dependent. To determine whether apoptosis mediated the growth inhibition observed in H460 cells treated with CTD, we performed an Annexin V-FITC/PI double-staining experiment and results are shown in Fig. 2D and E, a considerable increase in apoptotic cells was observed for H460 cells treated with CTD and these effects are time-dependent.

CTD induces DNA fragmentation in H460 cells. In order to delineate the mechanism of cell apoptosis mediated by CTD, we performed a DNA fragmentation assay, since DNA fragmentation is the characteristic for apoptosis. H460 cells were treated with 0, 5, 10 and 15 μM of CTD for 24 h and DNA was then isolated and analyzed by DNA agarose gel electrophoresis and the results are shown in Fig. 3. Fig. 3 indicates a typical ladder pattern of internucleosomal fragmentation was observed in cells after 24 h of CTD treatment. Low-molecular-weight DNA from these cells was resolved in 2.0% agarose gels (Fig. 3). These results suggest that CTD is a potent inducer of apoptosis in H460 cells.

CTD induces reactive oxygen species (ROS) and Ca^{2+} production and decreases the levels of mitochondrial membrane potential ($\Delta\Psi_m$) in H460 cells. To further examine the effects of CTD and whether it induced cell death in H460 cells through the production of Ca^{2+} or dysfunction of mitochondrial, the results from flow cytometric assay are shown in Fig. 4. Fig. 4A demonstrates that CTD decreased ROS from 1-12 h treatment. However, Fig. 4B indicates that CTD promoted the production of Ca^{2+} and these effects are time-dependent. Fig. 4C indicated that CTD decreased the levels of $\Delta\Psi_m$ and these effects are time-dependent. Fig. 4B shows that CTD promoted the Ca^{2+} release from 1 h up to 24 h treatment, however, the highest levels of Ca^{2+} release is in 6 h treatment. Both results indicated that CTD induced apoptosis of H460 cells is associated with dysfunction of mitochondria.

CTD promotes the mRNA expressions of caspase-3 and -8 in H460 cells. To further examine CTD promoting caspase-3 and -8 activities in H460 cells, and whether or not it was through the expression of mRNA of caspase-3 and -8, the cells were treated with CTD for 12 and 24 h and then isolated for total RNA followed by real-time PCR assay and the results are shown in Fig. 5. Data indicated that CTD promoted the gene expression of mRNA in caspase-3 and -8.

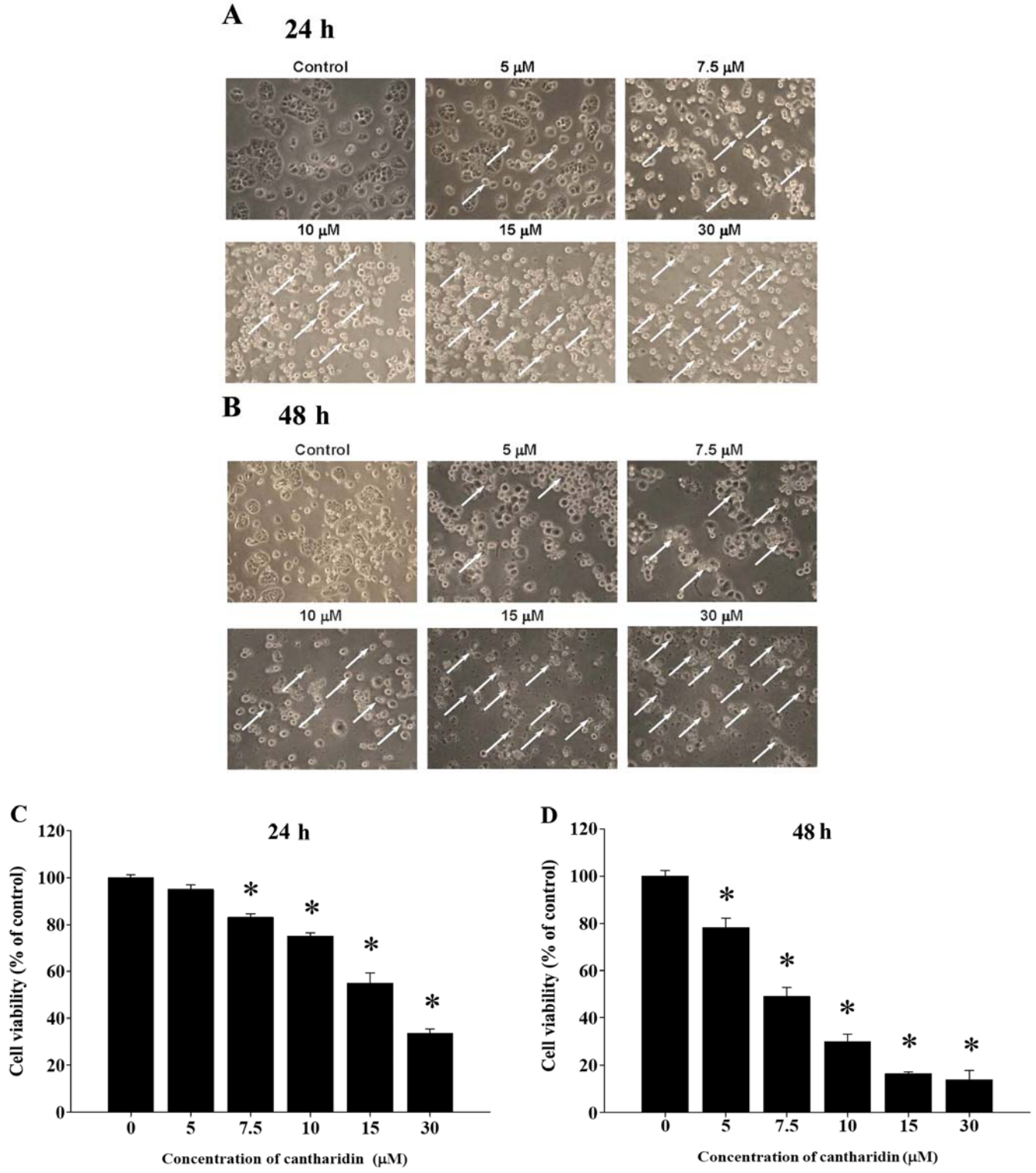

Figure 1. CTD induced cell morphological changes and decreased the percentage of viable H460 cells. H460 cells were treated with 0, 5, 7.5, 10, 15 and 30 μM of CTD for (A and C) 24 and (B and D) 48 h before the cells were examined and photographed for examining the cell morphological changes and were harvested for the percentage of viable cell determinations and analyzed by flow cytometry as described in Materials and methods. $^{*}p<0.05$, significant difference between CTD-treated groups and the control as analyzed by Student's t test.

CTD affects apoptosis-associated protein expression in H460 cells. For further examination on whether CTD induced apoptosis in H460 cells through the effects of apoptosis-associated protein, H460 cells were treated with 10 μM of CTD for 0, 6, 12, 24 and 48 h and then total proteins were quantitated and apoptosis-associated proteins were examined by western blot analysis and the results are shown in Fig. 6, indicated that CTD significantly promoted the expression of cleaved caspase-3 and -8, cytochrome *c*, Bax and AIF but inhibited the levels of Bcl-xL (Fig. 6A). Furthermore, CTD promoted ER stress- associated protein expression such as GRP78, IRE1α, IRE1β, ATF6α and caspase-4 (Fig. 6B). CTD promoted the

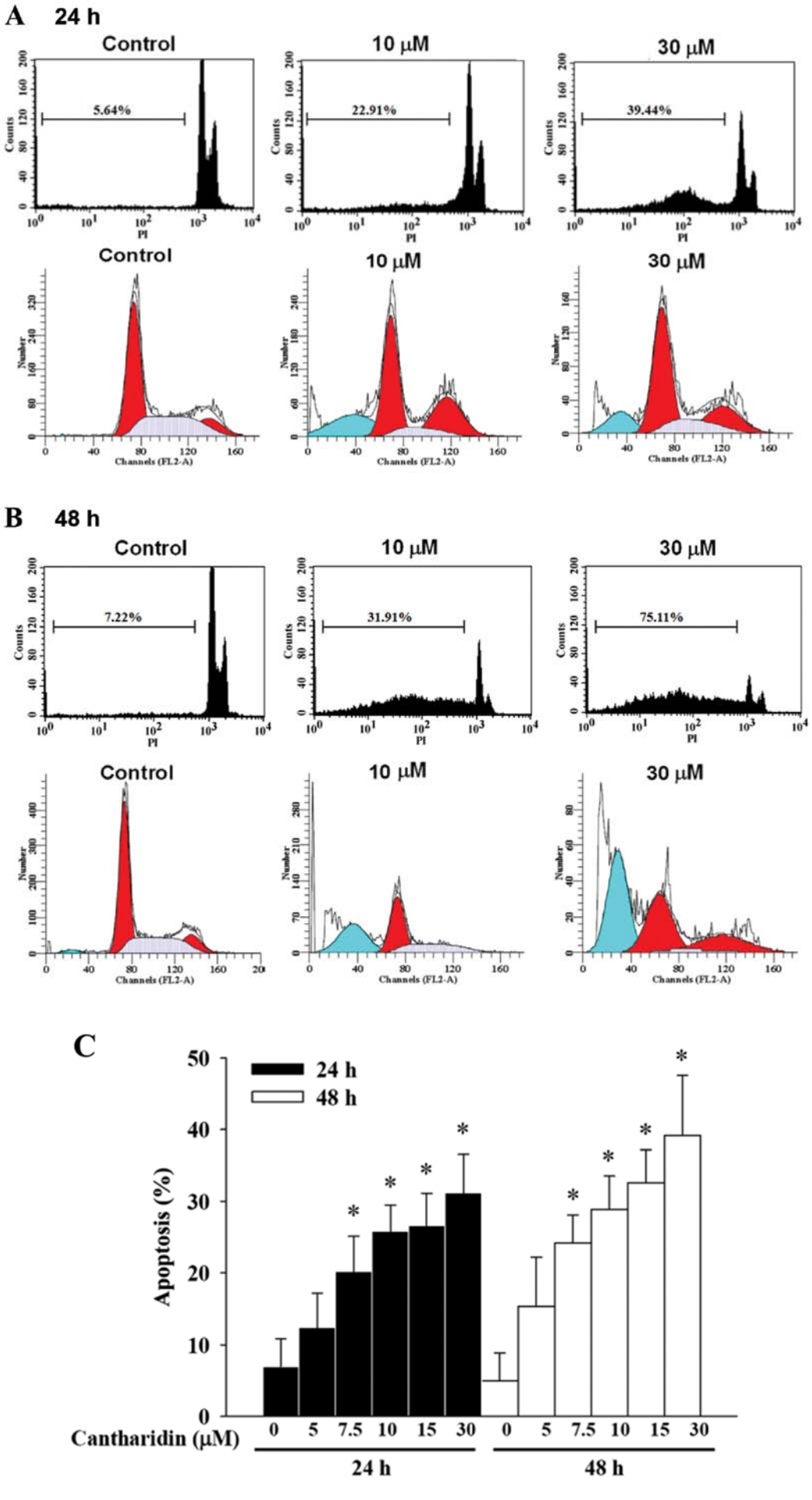
A 24 h
Control
10 μM
30 μM
5.64%
22.91%
39.44%
Counts
PI
Number
Channels (FL2-A)
B 48 h
7.22%
31.91%
75.11%
C
24 h
48 h
Apoptosis (%)
Cantharidin (μM)
0 5 7.5 10 15 30

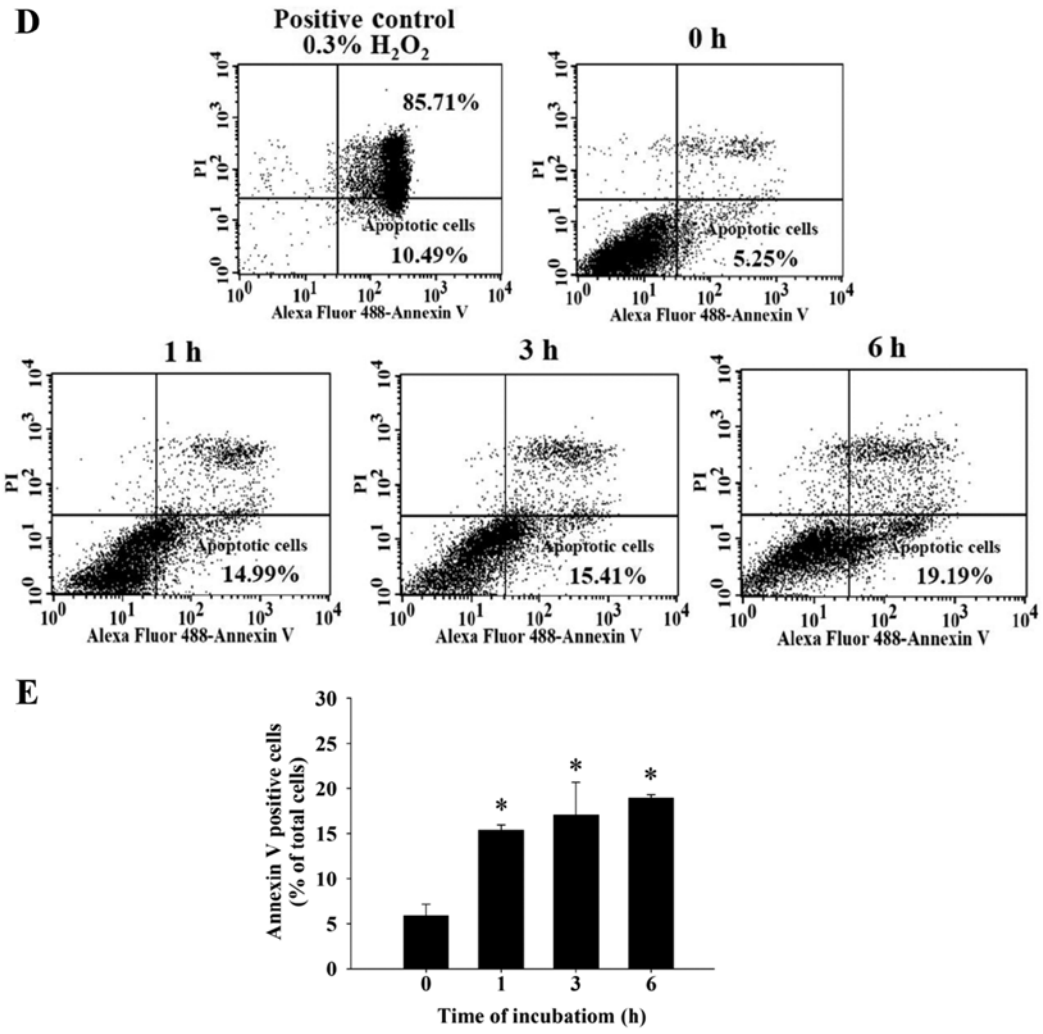

Figure 2. CTD induced sub-G1 phase and apoptosis of H460 cells. H460 cells were treated with 0, 5, 7.5, 10, 15 and 30 μM of CTD for 24 and 48 h before the cells were examined for sub-G1 phase of cell cycle (A, 24 h; B, 48 h; C, percentage of apoptotic cells) and also were stained by using (D) Annexin V-FITC/PI staining and (E) percentage of apoptotic cells and analyzed by flow cytometry as described in Materials and methods. *p<0.05, significant difference between CTD-treated groups and the control as analyzed by Student's t-test.

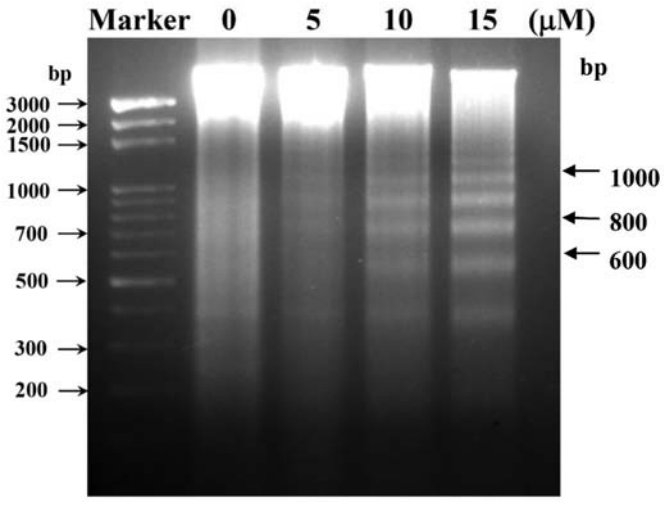

Figure 3. CTD induces DNA fragmentation in H460 cells. H460 cells were treated with 0, 5, 10 and 15 μM of CTD for 24 h before the cells were isolated for DNA and examined by DNA gel electrophoresis as described in Materials and methods.

expression of calpain 2 and XBP-1, but inhibited calpain 1 (Fig. 6C) that are associated with apoptosis pathways. These results indicated that CTD induced apoptosis in H460 cells through both caspase-dependent and -independent, ER stress and mitochondria-dependent pathways.

CTD affects the translocation of apoptotic-associated proteins in H460 cells. In order to confirm that CTD affects the translocation of cytochrome *c*, AIF and Endo G involved in apoptosis in H460 cells, cells were exposed to 10 μM of CTD for 24 h were then stained by anti-cytochrome *c*, AIF and Endo G and then were stained with secondary antibody and examined and photographed by confocal laser microscopy. The results are shown in Fig. 7, which indicated that CTD promoted the cytochrome *c* (Fig. 7A), AIF (Fig. 7B) and Endo G (Fig. 7C) release from mitochondria in H460 cells when compared to CTD untreated (control) groups.

Discussion

Substantial evidence shows that stimulating or inducing tumor cell apoptosis has been recognized to be a new possibility for

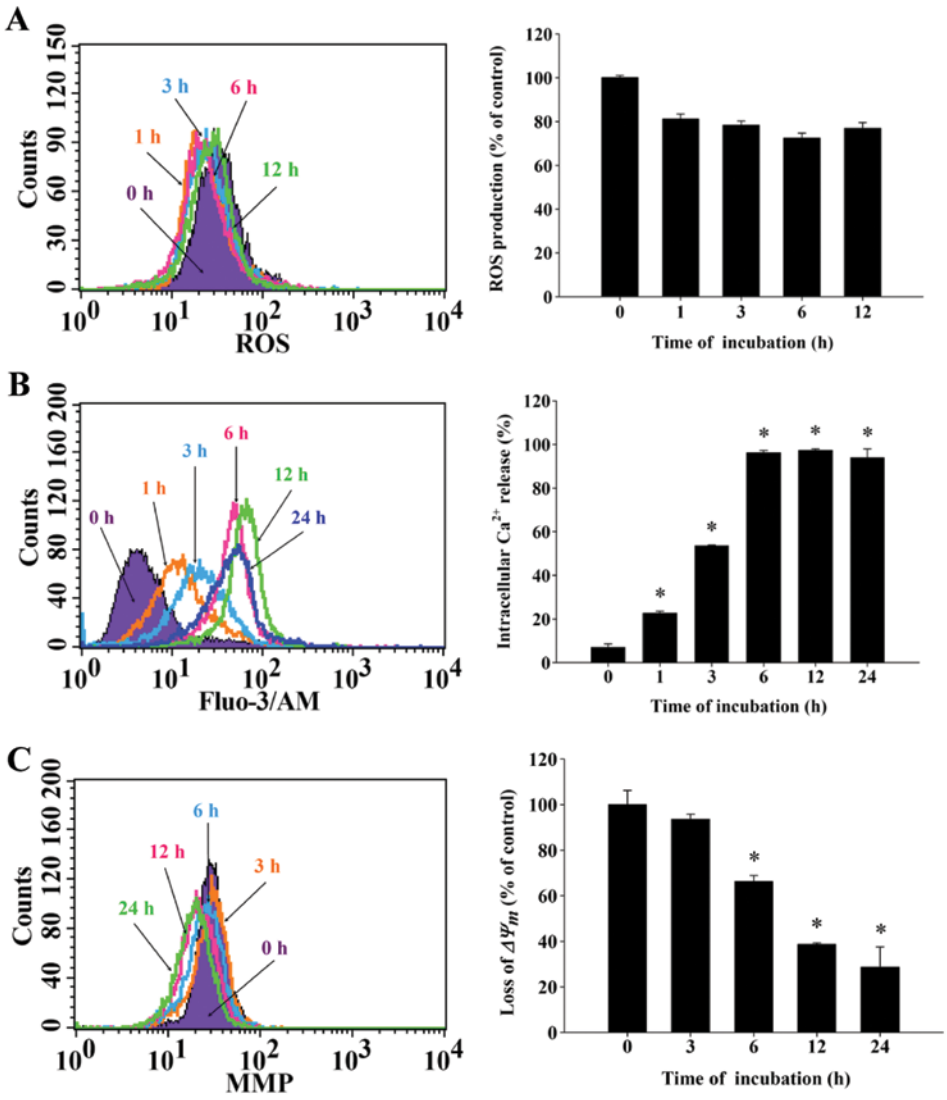

Figure 4. CTD induces ROS production, Ca^{2+} released and decreased the levels of $\Delta\Psi_m$ in H460 cells. H460 cells ($2x10^5$ cells/well) were treated with 10 μM of CTD for 0, 1, 3, 6, 12 or 24 h. All cells from each treatment and time point were isolated by centrifugation and were (A) re-suspended in 500 μl of DCFH-DA (10 μM) for 30 min for further ROS (H_2O_2), (B) re-suspended in 500 μl of Fluo-3/AM (2.5 μg/ml) for 30 min for further intracellular Ca^{2+} concentrations and (C) re-suspended in 500 μl of $DiOC_6$ (4 μmol/l) for 30 min for further study of the levels of $\Delta\Psi_m$ measurement as described in Materials and methods. The results are shown as a mean ± SD (n=3); *p<0.05, significant difference between CTD-treated groups and the control as analyzed by Student's t-test.

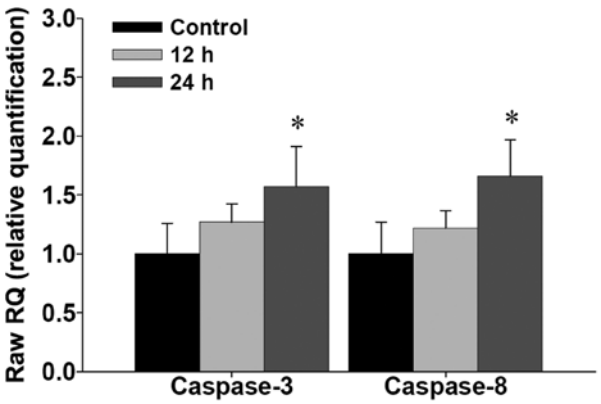

Figure 5. CTD promotes the mRNA expression of caspase-3 and -8 in H460 cells. Cells were treated with CTD for 12 and 24 h and then isolated with total RNA followed by real-time PCR assay as described in Materials and methods. Data indicated that CTD promoted the gene expression of mRNA in caspase-3 and -8. *p<0.05, significant difference between CTD-treated groups and the control as analyzed by Student's t-test.

tumor treatment. Although numerous studies have shown that CTD induced cell death and induction of apoptosis in many human cancer cells (5-12), there are no reports to show that CTD affected human lung cancer cells. Thus, herein, we investigated the effects of CTD on cell death of H460 human lung cancer cells *in vitro* and the results indicated that CTD induced cell morphological changes (Fig. 1A) and decreased the percentage of viable cells (Fig. 1B) via the induction of sub-G1 phase (apoptosis) (Fig. 2), which was examined and measured by flow cytometric assay. We also used DNA gel electrophoresis and Annexin V-FITC/PI staining for confirming H460 cell apoptosis which was induced by CTD. It is well documented that DNA fragmentation is one of the hallmarks of cell apoptosis (22,23), and in this study, we also isolated DNA from H460 cells with or without exposure to CTD, then DNA gel electrophoresis was performed and the result show increased doses led to increased DNA fragmentation (Fig. 3) which indicated that CTD induced apoptosis in H460 cells. We also

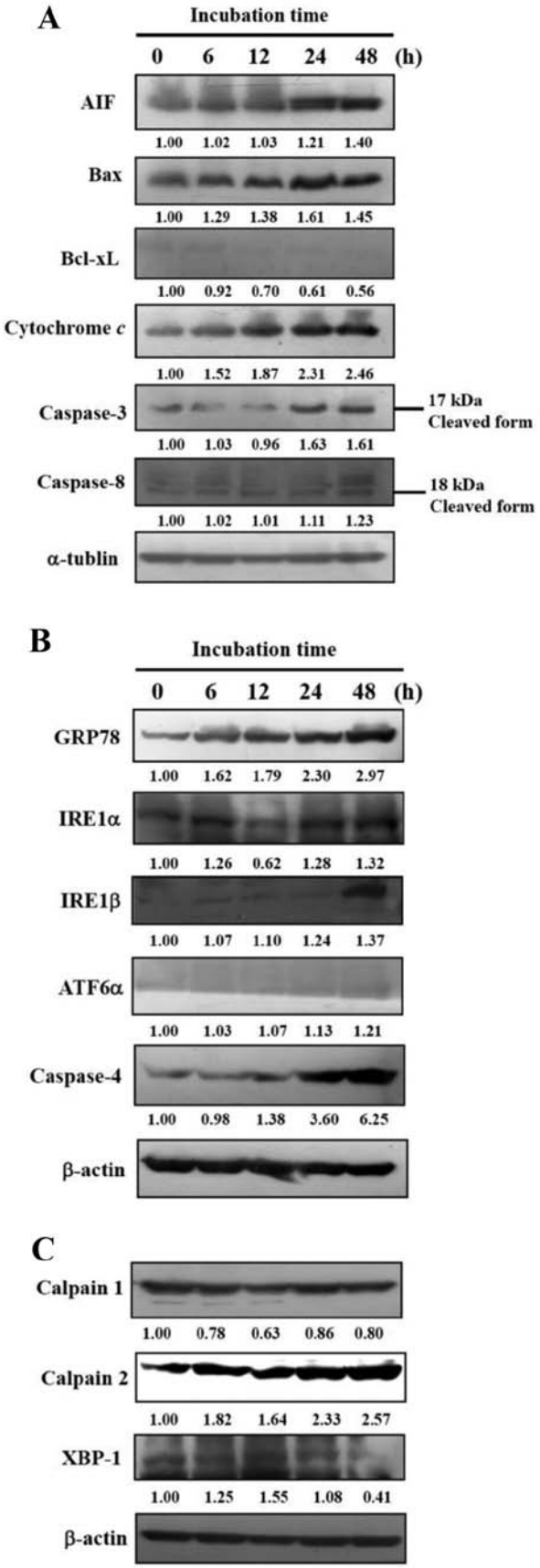

Figure 6. CTD affects apoptosis-associated protein expression in H460 cells. H460 cells were treated with 10 μM of CTD for 0, 6, 12, 24 and 48 h and then total proteins were quantitated and apoptosis-associated proteins were examined by western blot analysis as described in Materials and methods. (A) Caspase-3 and -8, cytochrome *c*, Bax, AIF and Bcl-xL. (B) GRP78, IRE1α, IRE1β, ATF6α and caspase-4. (C) Calpain 1, calpain 2 and XBP-1.

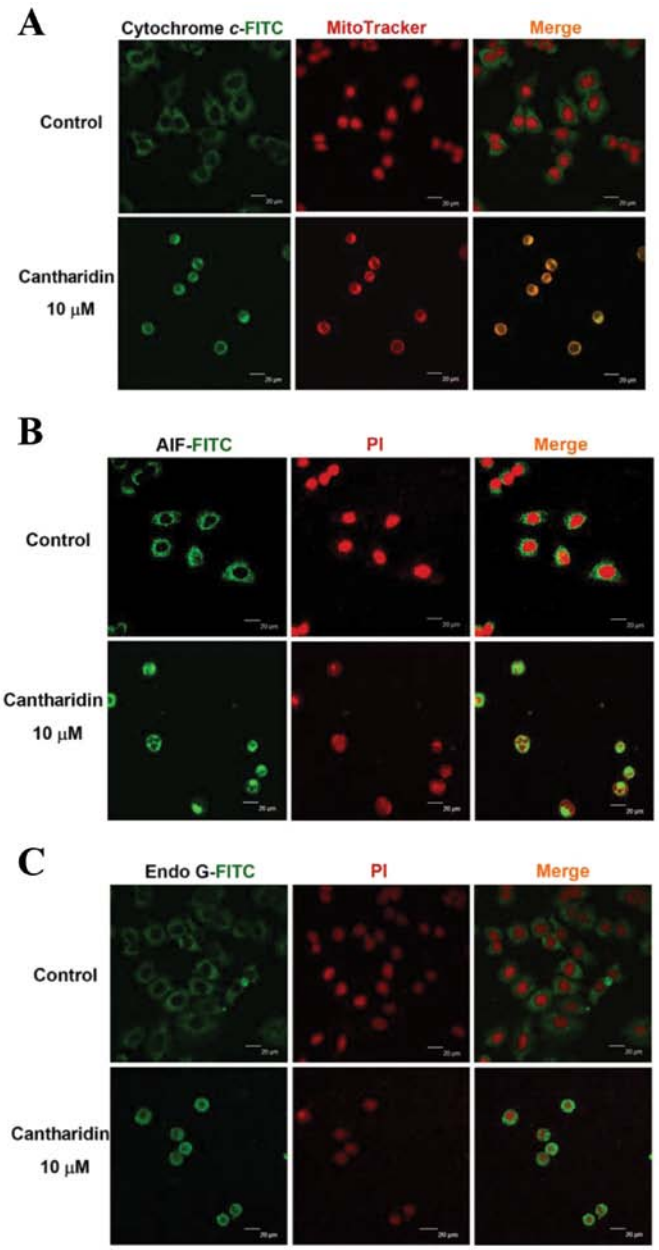

Figure 7. CTD affect the translocation of apoptosis-associated proteins in H460 cells. H460 cells were treated with 10 μM of CTD for 24 h and cells were stained by (A) anti-cytochrome *c*, (B) AIF and (C) Endo G and then were stained with secondary antibody FITC-conjugated goat anti-mouse IgG (green fluorescence) and were examined and photographed by a Leica TCS SP2 confocal laser microscopic systems as described in Materials and methods.

used Annexin V-FITC/PI staining for examining the cells and the results clearly demonstrated that CTD induced apoptosis in H460 cells (Fig. 2) and these effects are dose-dependent. Annexin V-FITC/PI staining is well accepted and widely used for measuring cell apoptosis (24,25).

To investigate the molecular mechanism including the signal pathway, we found that CTD promoted Ca^{2+} production and decreased the levels of $\Delta\Psi_m$ (Fig. 4B and C), and it also increased the mRNA expression of caspase-3 and -8 (Fig. 5). It is well known that apoptotic cell death can be regulated by either the extrinsic or the intrinsic apoptotic pathway (26-28). The extrinsic pathway is triggered by an agent connected with CD95 (also named Fas or Apo1) then involving caspase-8 activation

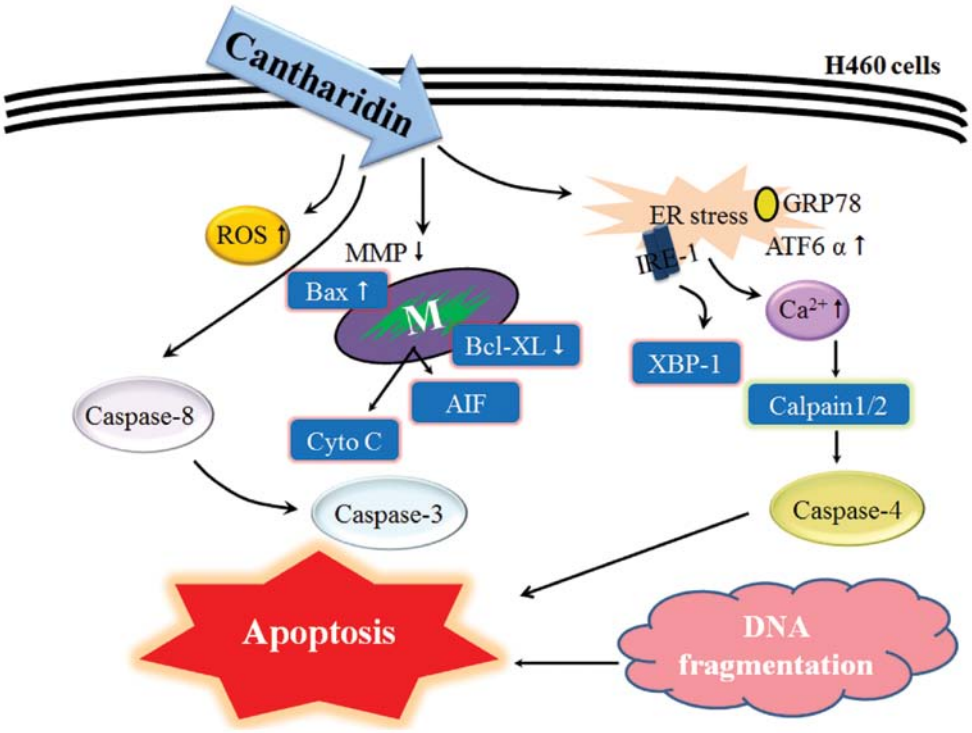

Figure 8. The possible signaling pathways for CTD-induced apoptosis in H460 cells.

leading to the activation of the downstream effector caspase-3 causing cell apoptosis (29). The intrinsic pathway involved in the dysfunction of mitochondria then led to the cytochrome *c* release, causing caspase-3 activation leading to apoptosis (30,31) or caused AIF and Endo G release from mitochondria directly inducing apoptosis (32,33). Based on these observations, we may suggest that CTD-induced cell apoptosis of H460 cells may be through the activation of caspase-3 and -8, and this is in agreement with our earlier report that CTD induced colon cancer cell apoptosis through caspase-dependent pathways (12). On the other hand it may also be through dysfunction of mitochondria base on the levels of $\Delta\Psi_m$ decrease and AIF and Endo G, which were increased as confirmed by western blot analysis (Fig. 6) and confocal laser microscopy examination (Fig. 7). This is in agreement with our earlier report that CTD induced bladder cancer cell apoptosis through mitochondria-dependent pathways (10). Numerous studies and evidence have demonstrated that agent-induced cancer cell apoptotic cell death are involved in caspase-dependent and -independent or mitochondria-dependent and -independent pathways (34,35). Herein, we may also suggest that CTD-induced apoptosis of H460 cells may be through caspase- and mitochondria-dependent pathways and also apoptosis through cross-talk between the extrinsic and the intrinsic pathways.

Based on the results from western blot analysis (Fig. 6), CTD increased the protein expression of Bax which is a pro-apoptotic protein and decreased the protein expression of Bcl-xL, which is an anti-apoptotic protein. It is reported that the ratio of Bax/Bcl-xL is associated with the changes of levels of mitochondria membrane potential $\Delta\Psi_m$ (36,37). Results in Fig. 4C also show that CTD decreased the levels of $\Delta\Psi_m$ as is obtained from flow cytometry assay. Based on the results (Fig. 7) from confocal microscopy examination, that CTD also promoted the release of cytochrome *c*, AIF and Endo G in H460 cells. These observations suggest that CTD induced apoptosis of H460 cells via mitochondria-dependent pathway. It was reported that CTD is an inhibitor of protein phosphatase 2A (PP2A) (8) and CTD also inhibits heat shock factor 1 (HSF1) transcriptional activity (38). Thus, for further investigation to identify the direct molecular targets of CTD other than PP2A, we will further explain its working mechanism.

In summary, in the present study, we suggest the possible significant molecular signal pathways for CTD inducing apoptosis in H460 cells as shown in Fig. 8. CTD may go through the death receptor (Fas receptor), activating caspase-8 following the activation of caspase-3 leading to apoptosis, or to increase the ratio of Bax/Bcl-xL leading to dysfunction of mitochondria (decrease the levels of $\Delta\Psi_m$) causing cytochrome *c*, AIF and Endo G release then leading to apoptosis.

Acknowledgements

This study was supported by grant CMU 101-AWARD-03(1/2) from China Medical University, Taichung, Taiwan, R.O.C.

References

1. Parkin DM, Bray F, Ferlay J and Pisani P: Global cancer statistics, 2002. CA Cancer J Clin 55: 74-108, 2005.
2. Parlak C, Mertsoylu H, Guler OC, Onal C and Topkan E: Definitive chemoradiation therapy following surgical resection or radiosurgery plus whole-brain radiation therapy in non-small cell lung cancer patients with synchronous solitary brain metastasis: a curative approach. Int J Radiat Oncol Biol Phys 88: 885-891, 2014.
3. Salama JK, Pang H, Bogart JA, *et al*: Predictors of pulmonary toxicity in limited stage small cell lung cancer patients treated with induction chemotherapy followed by concurrent platinum-based chemotherapy and 70 Gy daily radiotherapy: CALGB 30904. Lung Cancer 82: 436-440, 2013.

4. Xu B: The influence of several anticancer agents on cell proliferation, differentiation and the cell cycle of murine erythroleukemia cells. Am J Chin Med 9: 268-276, 1981.
5. Wang CC, Wu CH, Hsieh KJ, Yen KY and Yang LL: Cytotoxic effects of cantharidin on the growth of normal and carcinoma cells. Toxicology 147: 77-87, 2000.
6. Sagawa M, Nakazato T, Uchida H, Ikeda Y and Kizaki M: Cantharidin induces apoptosis of human multiple myeloma cells via inhibition of the JAK/STAT pathway. Cancer Sci 99: 1820-1826, 2008.
7. Li W, Chen Z, Zong Y, *et al*: PP2A inhibitors induce apoptosis in pancreatic cancer cell line PANC-1 through persistent phosphorylation of IKKalpha and sustained activation of the NF-kappaB pathway. Cancer Lett 304: 117-127, 2011.
8. Li W, Xie L, Chen Z, *et al*: Cantharidin, a potent and selective PP2A inhibitor, induces an oxidative stress-independent growth inhibition of pancreatic cancer cells through G2/M cell-cycle arrest and apoptosis. Cancer Sci 101: 1226-1233, 2010.
9. Huan SK, Lee HH, Liu DZ, Wu CC and Wang CC: Cantharidin-induced cytotoxicity and cyclooxygenase 2 expression in human bladder carcinoma cell line. Toxicology 223: 136-143, 2006.
10. Kuo JH, Chu YL, Yang JS, *et al*: Cantharidin induces apoptosis in human bladder cancer TSGH 8301 cells through mitochondria-dependent signal pathways. Int J Oncol 37: 1243-1250, 2010.
11. Williams LA, Moller W, Merisor E, Kraus W and Rosner H: In vitro anti-proliferation/cytotoxic activity of cantharidin (spanish fly) and related derivatives. West Indian Med J 52: 10-13, 2003.
12. Huang WW, Ko SW, Tsai HY, *et al*: Cantharidin induces G2/M phase arrest and apoptosis in human colorectal cancer colo 205 cells through inhibition of CDK1 activity and caspase-dependent signaling pathways. Int J Oncol 38: 1067-1073, 2011.
13. Huan SK, Wang KT, Yeh SD, *et al*: *Scutellaria baicalensis* alleviates cantharidin-induced rat hemorrhagic cystitis through inhibition of cyclooxygenase-2 overexpression. Molecules 17: 6277-6289, 2012.
14. Coloe Dosal J, Stewart PW, Lin JA, Williams CS and Morrell DS: Cantharidin for the treatment of *Molluscum contagiosum*: a prospective, double-blinded, placebo-controlled trial. Pediatr Dermatol: Aug 16, 2012 (Epub ahead of print).
15. Yu ZJ: Chinese material medica combined with cisplatin and lipiodol through transcatheter arterial embolization in the treatment of primary hepatoma. Zhongguo Zhong Xi Yi Jie He Za Zhi 13: 327-329, 323, 1993 (In Chinese).
16. Chen YH, Hung MC and Shyu WC: Role of cancer stem cells in brain tumors. BioMedicine 2: 84-91, 2012.
17. Lin YT, Huang AC, Kuo CL, *et al*: Induction of cell cycle arrest and apoptosis in human osteosarcoma U-2 OS cells by *Solanum lyratum* extracts. Nutr Cancer 65: 469-479, 2013.
18. Chueh FS, Chen YL, Hsu SC, *et al*: Triptolide induced DNA damage in A375.S2 human malignant melanoma cells is mediated via reduction of DNA repair genes. Oncol Rep 29: 613-618, 2013.
19. Li CC, Lo HY, Hsiang CY and Ho TY: DNA microarray analysis as a tool to investigate the therapeutic mechanisms and drug development of Chinese medicinal herbs. BioMedicine 2: 10-16, 2012.
20. Yu FS, Huang AC, Yang JS, *et al*: Safrole induces cell death in human tongue squamous cancer SCC-4 cells through mitochondria-dependent caspase activation cascade apoptotic signaling pathways. Environ Toxicol 27: 433-444, 2012.
21. Ho YT, Lu CC, Yang JS, *et al*: Berberine induced apoptosis via promoting the expression of caspase-8, -9 and -3, apoptosis-inducing factor and endonuclease G in SCC-4 human tongue squamous carcinoma cancer cells. Anticancer Res 29: 4063-4070, 2009.
22. Huang CY and Lee SD: Possible pathophysiology of heart failure in obesity: Cardiac apoptosis. BioMedicine 2: 36-40, 2012.
23. Momtazi-Borojeni AA, Behbahani M and Sadeghi-Aliabadi H: Antiproliferative activity and apoptosis induction of crude extract and fractions of avicennia marina. Iran J Basic Med Sci 16: 1203-1208, 2013.
24. Ji BC, Yu CC, Yang ST, *et al*: Induction of DNA damage by deguelin is mediated through reducing DNA repair genes in human non-small cell lung cancer NCI-H460 cells. Oncol Rep 27: 959-964, 2012.
25. Yin MC: Anti-glycative potential of triterpenes: A mini-review. BioMedicine 2: 2-9, 2012.
26. Igney FH and Krammer PH: Death and anti-death: tumour resistance to apoptosis. Nat Rev Cancer 2: 277-288, 2002.
27. Kumar S: Caspase function in programmed cell death. Cell Death Differ 14: 32-43, 2007.
28. Xu G and Shi Y: Apoptosis signaling pathways and lymphocyte homeostasis. Cell Res 17: 759-771, 2007.
29. Wilson MR: Apoptotic signal transduction: emerging pathways. Biochem Cell Biol 76: 573-582, 1998.
30. Cory S and Adams JM: The Bcl2 family: regulators of the cellular life-or-death switch. Nat Rev Cancer 2: 647-656, 2002.
31. Newmeyer DD and Ferguson-Miller S: Mitochondria: releasing power for life and unleashing the machineries of death. Cell 112: 481-490, 2003.
32. Liu W, Fan Z, Han Y, Zhang D, Li J and Wang H: Intranuclear localization of apoptosis-inducing factor and endonuclease G involves in peroxynitrite-induced apoptosis of spiral ganglion neurons. Neurol Res 34: 915-922, 2012.
33. Kapoor R, Rizvi F and Kakkar P: Naringenin prevents high glucose-induced mitochondria-mediated apoptosis involving AIF, Endo-G and caspases. Apoptosis 18: 9-27, 2013.
34. Chueh FS, Hsiao YT, Chang SJ, *et al*: Glycyrrhizic acid induces apoptosis in WEHI-3 mouse leukemia cells through the caspase- and mitochondria-dependent pathways. Oncol Rep 28: 2069-2076, 2012.
35. Lin PC, Liu PY, Lin SZ and Harn HJ: Angelica sinensis: A Chinese herb for brain cancer therapy. BioMedicine 2: 30-35, 2012.
36. Goloudina AR, Mazur SJ, Appella E, Garrido C and Demidov ON: Wip1 sensitizes p53-negative tumors to apoptosis by regulating the Bax/Bcl-xL ratio. Cell Cycle 11: 1883-1887, 2012.
37. Liu FT, Goff LK, Hao JH, Newland AC and Jia L: Increase in the ratio of mitochondrial Bax/Bcl-XL induces Bax activation in human leukemic K562 cell line. Apoptosis 9: 377-384, 2004.
38. Kim JA, Kim Y, Kwon BM and Han DC: The natural compound cantharidin induces cancer cell death through inhibition of heat shock protein 70 (HSP70) and Bcl-2-associated athanogene domain 3 (BAG3) expression by blocking heat shock factor 1 (HSF1) binding to promoters. J Biol Chem 288: 28713-28726, 2013.